Kalman Filter Based Estimation of Neutral Axis Position of Bridge Deck under Traffic Loading

H. W. XIA* Y. Q. NI* and X. W. YE*
*Department of Civil and Structural Engineering, The Hong Kong Polytechnic University, Hung Hom, Kowloon, Hong Kong
E-mail: HW.Xia@polyu.edu.hk; Yiqing.Ni@inet.polyu.edu.hk; cexwye@polyu.edu.hk

Abstract
In recognizing that small structural defects could be often discerned from the variation in strain or its derivatives rather than in acceleration, strain-based methods for structural damage detection have received increasing attention recently. In this study, the neutral-axis position of bridge deck cross-sections is proposed as a damage indicator for bridge deck assessment and a Kalman filter (KF) based method for optimal estimation of the neutral-axis position from dynamic strain measurement data under operational traffic is developed. As observed from the monitoring data, under traffic effect, bridge deck performs like a flexural beam, i.e., the deck top compresses and the deck bottom extends concurrently, or vice versa. Based on the relationship between the neutral-axis position and strain response, a KF estimator for locating the neutral-axis position is formulated and used to verify its robustness to noise disturbance through numerical simulations. The numerical studies show that the estimator generates satisfactory results in the presence of noise. The proposed KF estimator is further applied for neutral-axis estimation of the suspension Tsing Ma Bridge (TMB) using long-term monitoring data of dynamic strain responses. The results show that the neutral-axis position is insensitive to the traffic environment and hence can serve as an indicator for deck condition assessment.

Key words: Bridge deck, Neutral-axis estimation, Dynamic strain, Kalman filter, Condition assessment

1. Introduction

Because of its live load carrying capacity, bridge deck is one of the most critical parts of a bridge system, which directly carries the traffic. Bridge deck is deteriorating at an ever-increasing number and pace according to the FHWA report[(1)]. Usually the obsolescence results from traffic load increasing, harsh environment attacking, or other adverse changes in the use of the structure. Deterioration of bridge deck can cause public inconvenience, travel delay, economic impact, and even life lost, giving rise to the most severe problem for highway industry today. A cost-effective approach to preventing this problem is the use of monitoring technologies to collect data pertaining to the condition of in-service bridge deck. Such precautionary work can be done before more serious situation arises or catastrophe happens.

Under traffic loading environment, cracks are prone to occur in beam-like bridge deck. Crack damage can heavily affect the global safety and performance of in-service bridges, and more severely, continual operation without noticing the damage accumulation will be disastrous. To understand bridge deck failure mechanism, numerous studies of crack damage detections have been carried out on beam-like structures in laboratory[(2),(3),(4)]. Kim

conducted an experimental investigation of saw-cut damage on the 1/15 scale model of a suspension bridge deck[5]. In his study, the signal anomaly index was proposed as an indicator of damage. Park et al. presented a strain-flexibility based crack detection method for a steel beam[6]. An experimental study was carried out by Lee et al. on a cracked cantilever beam to verify their proposed neural-network method for structural damage detection[7]. Although the above methods achieved a certain success with simulation and laboratory data, they still have limitations in application to field monitoring data. Catbas and Aktan indicated that it is possible to extract the actual unit influence line (UIL) of a bridge deck for damage detection[8]. Online evaluation of UIL under normal traffic environment is envisioned as long as the limitations of signal decomposition are clearly understood and mitigated. However, UIL based damage detection methods may encounter the same problem of damage sensitivity as vibration based approaches have. Zhu and Law presented a wavelet-based method for crack detection under moving load condition[9]. A dip of wavelet coefficients of one measurement signal was used as an indication of damage happening on a test beam. However, anomalies of the wavelet coefficient may be due to varying load patterns, which are not related to damage.

In selection of damage indices for bridge deck assessment, their sensitivity to damage and robustness with respect to different traffic load patterns should be taken into consideration. Theoretically the neutral-axis position of a bridge deck section remains unchanged under the varying traffic environment. In addition, it has potential in improving the sensitivity to damage because it reflects the local cross-section property. This study is to propose the neutral-axis position as an indicator of damage for deck condition assessment and develop an estimation method to locate the neutral-axis position from traffic-induced strains. Based on the bending behavior, a KF estimator is formulated and then numerical simulations are conducted to verify its capability of anti-disturbance in noise contamination. Finally application of the verified KF estimator to TMB for deck condition assessment is carried out.

2. Structural Behavior of Beam-like Deck

Generally long-span bridge deck behaves like a bending beam because the cross section under eccentric loads has relatively little influence on the principal bending strain or stress responses. In the elastic theory of beams, it is assumed that the plane sections remain plane when deforming, and that the beam is composed of discrete linear fibers. From the assumption it can be shown that, at any point on a cross section, the longitudinal strain ε is proportional to the distance y of the point from the neutral axis, which passes through the centroid of the section. As shown in Figure 1, strains at the bottom and top locations of the section are denoted by ε_b and ε_t, respectively. Following the geometric relation, the ratio of ε_b and ε_t can be expressed as

$$\frac{\varepsilon_t}{\varepsilon_b} = \frac{y_t}{y_b} \quad or \quad \frac{\varepsilon_t}{\varepsilon_t + \varepsilon_b} = \frac{y_t}{y_t + y_b} \tag{1}$$

where y_t is the distance between the top and the neutral axis, and y_b is the distance between the bottom and the neutral axis. The ratio defined in Equation (1) is equivalent to that of the neutral-axis location over the height of the cross section:

$$\frac{y_t}{y_t + y_b} = \frac{y_n}{h} = r \tag{2}$$

where y_n denotes the neutral-axis location of the cross section, h is the height of the cross section.

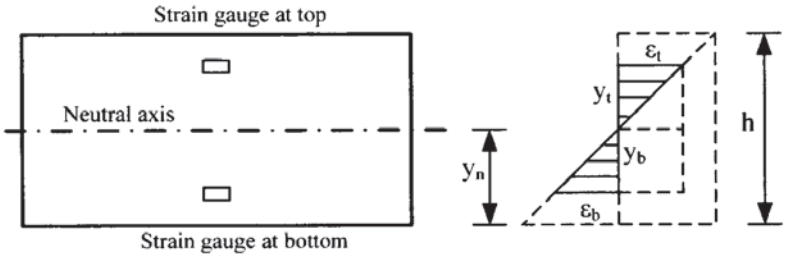

Fig. 1 Flexural strain distribution over depth of cross section.

3. Neutral-Axis Position Estimation

3.1 Direct estimation method

Under traffic loadings, bending behavior dominates the response of beam-like deck. The neutral-axis position can be estimated by

$$\hat{r} = \frac{\varepsilon_b}{\varepsilon_t + \varepsilon_b} \tag{3}$$

if the strain responses at top and bottom points are measured. But its efficiency can only be ensured on the condition that the measurement data are free of noise contamination.

3.2 KF based estimation method

The Kalman filter is a mathematical method named after Kalman[10]. It is purposed to use measurements observed over time (containing noise and other inaccuracies) to produce values that tend to be closer to the true values of the measurements. Theoretically Kalman filter combines a system's dynamic model (i.e., physical laws of motion) and measurements (i.e., sensor readings) to form an estimate of the system's varying quantities (its state) that is better than the estimate obtained by measurement alone. It is similar in many respects to the least-square approach to estimation and, in a sense, the Kalman filter can be regarded as a generalization of the least-square method. A salient advantage of the Kalman filter is that the assumption of stationarity of the model coefficients can be relaxed.

In this study, the neutral-axis position in ratio ($r = y_n/h$) is taken as the state variable to be estimated. Because there is no deterministic disturbance or control scalar, the discrete model of the chosen state is given by

$$r_k = \Phi_k r_{k-1} + w_k \tag{4}$$

where Φ_k is the propagation scalar that propagates the state from one sampling instant to the next and w_k is the white process noise. And the measurement equation is given as

$$z_k = H r_k + v_k \tag{5}$$

where H is the measurement scalar that relates the state to the observation z_k, and v_k is the measurement noise. In this special case the discrete Kalman filtering equation simplifies to

$$\hat{r}_k = \Phi_k \hat{r}_{k-1} + K_k(z_k - H\Phi_k \hat{r}_{k-1}) \tag{6}$$

From the preceding equations, the error in the estimate is

$$\tilde{r}_k = r_k - \hat{r}_k = r_k - \Phi_k \hat{r}_{k-1} - K_k(z_k - H\Phi_k \hat{r}_{k-1}) \tag{7}$$

Recognizing that the measurement can be expressed in terms of the state, Equation (7) can be formulated as

$$\tilde{r}_k = r_k - \hat{r}_k = r_k - \Phi_k \hat{r}_{k-1} - K_k(Hr_k + v_k - H\Phi_k \hat{r}_{k-1}) \tag{8}$$

Noting that the state at time k can be replaced by an alternate expression at time k-1, it is obtained that

$$\tilde{r}_k = r_k - \hat{r}_k = r_k - \Phi_k \hat{r}_{k-1} - K_k(H\Phi_k r_{k-1} + Hw_k + v_k - H\Phi_k \hat{r}_{k-1}) \tag{9}$$

Because

$$\tilde{r}_k = r_k - \hat{r}_k \tag{10}$$

it also says that

$$\tilde{r}_{k-1} = r_{k-1} - \hat{r}_{k-1} \tag{11}$$

Therefore, combining the similar terms in the error estimation equation yields

$$\tilde{r}_k = (1 - K_k H)\tilde{r}_{k-1}\Phi_k + (1 - K_k H)w_k - K_k v_k \tag{12}$$

If the covariance of estimate error is defined as

$$P_k = E(\tilde{r}_k^2) \tag{13a}$$

and similarly

$$Q_k = E(w_k^2) \tag{13b}$$

$$R_k = E(v_k^2) \tag{13c}$$

then by squaring and taking expectations of both sides of Equation (12) yields

$$P_k = (1 - K_k H)^2 (P_{k-1}\Phi_k^2 + Q_k) + K_k^2 R_k \tag{14}$$

By defining

$$M_k = P_{k-1}\Phi_k^2 + Q_k \tag{15}$$

then the covariance equation becomes

$$P_k = (1 - K_k H)^2 M_k + K_k^2 R_k \tag{16}$$

The Kalman filter gain K_k that minimizes the variance of the error in the estimate can be found by simply taking the derivative of the preceding expression with respect to the gain and setting the result equal to zero, that is

$$\frac{\partial P_k}{\partial K_k} = 2(1 - K_k H)M_k(-H) + 2K_k R_k \tag{17}$$

Solving the preceding equation for the gain yields

$$K_k = \frac{M_k H}{H^2 M_k + R_k} = M_k H (H^2 M_k + R_k)^{-1} \tag{18}$$

Substitution of the optimal gain into the covariance equation yields

$$P_k = \frac{R_k M_k}{H^2 M_k + R_k} = \frac{R_k K_k}{H} \tag{19}$$

By inverting the optimal gain equation, it obtains

$$K_k R_k = M_k H - H^2 M_k K_k \tag{20}$$

Substituting the preceding equation back into the variance equation yields

$$P_k = \frac{R_k K_k}{H} = \frac{M_k H - H^2 M_k K_k}{H} = M_k - H M_k K_k \tag{21}$$

or, more simply,

$$P_k = (1 - K_k H)M_k \tag{22}$$

The above derivation shows that the gain of the Kalman filter is chosen to minimize the variance of the error in the estimate. An iterative way of finding the optimal gain at each step is illustrated in Equations (15), (18) and (22).

3.3 Performance analysis

In the previous section, based on the relation between the neutral-axis position and strain responses, a KF estimator for locating the neutral-axis position from strain measurements has been derived. The verification of its stability to noise contamination by numerical simulation comes in this section. Dynamic strain response data are first produced by finite element (FE) simulation of a flexural beam under moving load. Simulated strain responses at the top and bottom of a cross section are illustrated in Figure 2. It is shown that the strain responses at the top and bottom points evolve with time in almost same amplitudes but opposite directions, which favorably demonstrates the bending behavior. Compared with the free of noise case, the strain responses with 5% noise are not smooth any more with some small wavelets on them. As to the 10% noise case, it is observed that the strain time histories fluctuate more seriously in comparison to those of 5% noise case.

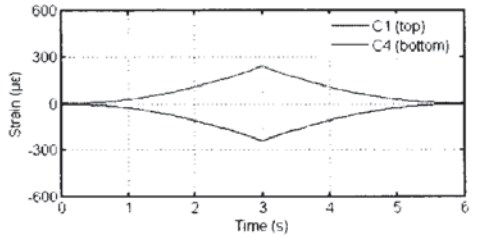

(a) no noise

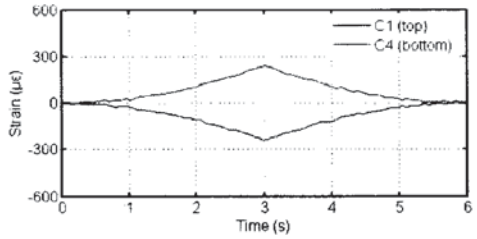

(b) 5% noise

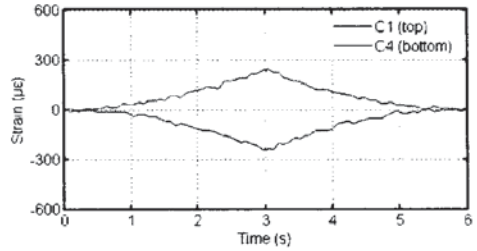

(c) 10% noise

Fig. 2 Simulated strain responses at top and bottom of section C.

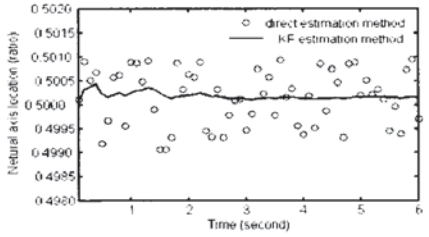

(a) no noise

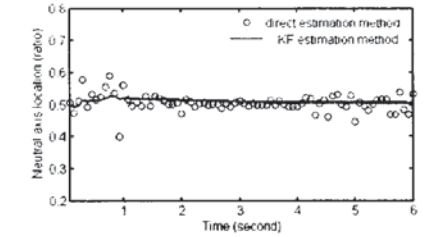

(b) 5% noise

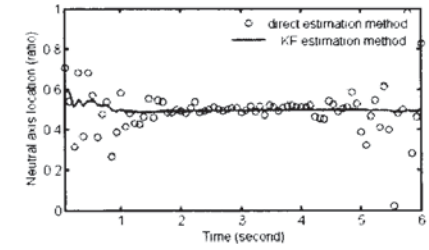

(c) 10% noise

Fig. 3 Comparison between direct and KF estimation methods.

Table 1 Performance analysis of KF estimator for simulation data

Simulation cases	Direct method		KF method
	mean	standard deviation	
Case 1	0.5001565	5.78e-4	0.5001539
Case 2	0.5005189	0.0258	0.5002154
Case 3	0.4984721	0.1156	0.4995412

The performance of the direct and KF methods is evaluated. As illustrated in Figure 3, when there is no noise contamination, the KF estimator has a perfect performance. When 5% noise is corrupted, the performance of the KF estimator degrades at the beginning but after a while the estimation converges to the true value. As to the more noisy case with 10% noise contamination, the fluctuation becomes more serious at the beginning of the estimation process. But with the iteration going further, convergence is achieved as expected. A comparison of the results in the three cases is provided in Table 1. In Case 1, the direct and KF estimation methods both reach the true value of 0.5. Their relative errors are 0.0313% and 0.0308%, respectively. The standard deviation of the direct estimation results is as small as 5.78E-04, demonstrating its efficiency when there is no noise. However, with the increase of noise level, the estimation results by the direct method deteriorate seriously such that the relative error goes to 0.1038% and -0.3056% in Case 2 and Case 3, respectively. The standard deviation increases obviously, indicating that the direct estimation results are not reliable. Contrarily, the KF approach achieves improved

estimates, evidenced by the relative error of 0.0431% in Case 2 and -0.0918% in Case 3. These results demonstrate that the KF estimator has an excellent anti-disturbance ability in noise contamination.

4. Application to TMB Deck Assessment

The deck of TMB is a double-deck box with truss stiffening and non-structural edge fairing as shown in Figure 4[11]. The longitudinal diagonally braced trusses on the north and south sides of the cross-section consist of top chords, diagonal struts and bottom chords. All truss components on selected cross-sections have been instrumented with strain gauges (single, pair and rosette strain sensors). The strain data were acquired at sampling rates of 25.6 Hz and 51.2 Hz, respectively. Strain responses of the deck trusses are monitored and recorded continuously.

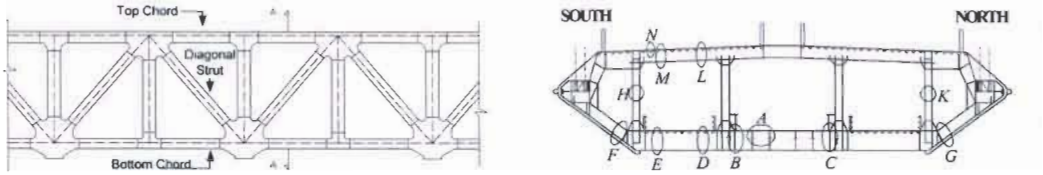

(a) elevation view (b) cross-section view

Fig. 4 Truss deck of TMB.

In TMB, the in-service monitoring data of strain acquired from the deck trusses stem mainly from four effects: highway traffic, railway traffic, wind, and temperature (the static strain due to initial dead loads is unable to obtain as the strain gauges were installed after the completion of construction). The traffic-induced strain components reveal the bending behavior very well either in highway or railway traffic[12]. Figure 5 illustrates the extracted traffic-induced strains experienced by a top chord and a bottom chord on the deck section CH24662.50 for a typical day. It is observed that the magnitude of the strain responses acquired at 2:00 to 5:00 am is relatively small since railway traffic ceases to operate during that period. This observation proposes that the strain responses are sensitive to traffic load patterns.

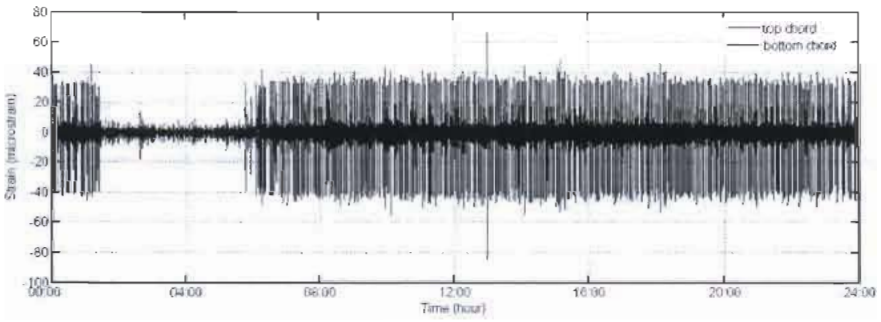

Fig. 5 Traffic-induced strain time histories experienced by top and bottom chords.

Theoretically, the neutral-axis position of the bridge deck section does not change under the varying traffic environment. It will be testified in this section. Four typical load patterns are observed in Figure 5 and grouped as follows: (1) 00:00~02:00; (2) 03:00~05:00; (3) 05:00~07:00; (4) 10:00~12:00. The KF approach to the neutral-axis position estimation is applied on these strain measurement data. As an example, Figure 6(a) illustrates the extracted strain response data during the time period of 00:00~02:00, which include a transition of traffic pattern from having to not having railway traffic. Although this transition pattern is remarkably reflected in the strain responses, it does not affect the neutral-axis position estimated by the KF approach as shown in Figure 6(b).

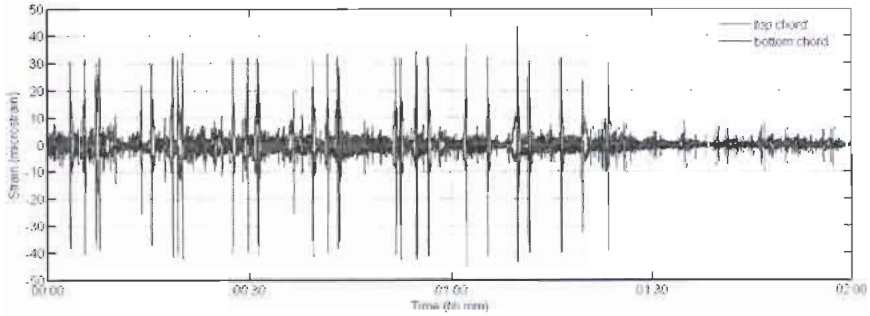

(a) traffic-induced strain time histories

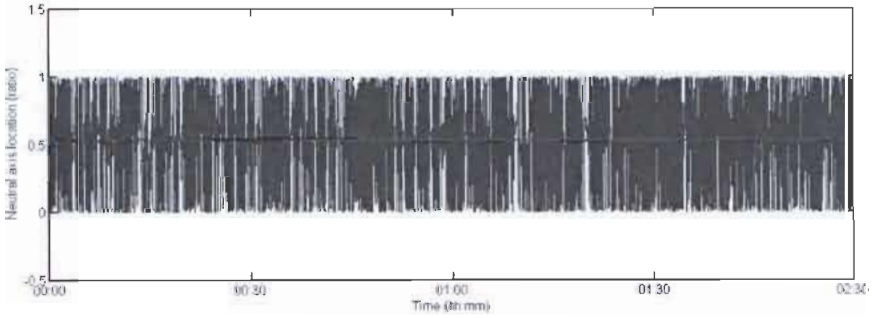

(b) estimated neutral-axis position by direct and KF methods

Fig. 6 Traffic-induced strain time histories and estimated neutral-axis position (00:00~02:00).

Table 2 Comparison of estimated neutral-axis position of TMB deck under different load patterns

Time period	Direct method		KF method
	mean	standard deviation	
00:00~02:00	0.5423851	0.2127	0.5423849
03:00~05:00	0.5476296	0.2348	0.5476295
05:00~07:00	0.5425675	0.2071	0.5425693
10:00~12:00	0.5408021	0.2044	0.5408047
00:00~24:00	0.5438627	0.1968	0.5438627

Estimation results for different time periods are listed in Table 2. The variation range of the estimation mean by the direct method is between 0.5408021 and 0.5476296, but the standard deviation is remarkable. Contrarily the KF method has a stable performance during the estimation process. The estimation results vary in the range of 0.5408047 to 0.5476295. They fluctuate between -0.49% and 0.77% of their mean value.

5. Conclusions

It is observed from the field monitoring data that the TMB bridge deck performs like a flexural beam, i.e., the deck top compresses and the deck bottom tensions concurrently, or vice versa. Based on the bending behavior, a KF estimator of locating the neutral-axis position from the strain measurement is formulated. Its capability of anti-disturbance in noise contamination has been testified by numerical studies. Further the proposed KF estimator has been applied to the strain measurement data acquired from the TMB deck. The following observations have been made: (1) The variation range of the estimation mean by the direct method is between 0.5408021 and 0.5476296, but the standard deviation is remarkable, indicating the direct estimation results are not reliable; (2) The KF method has a stable performance under different load patterns and the estimation results vary in the range of 0.5408047 to 0.5476295, which fluctuate between -0.49% and 0.77% of their mean value. It is therefore concluded that the neutral-axis position of the bridge deck cross section

does not change under the varying traffic environment, and hence can serve as an indicator for deck condition assessment.

References

(1) FHWA, Bridge scour and stream instability countermeasure experience, selection, and design guidance, Federal Highway Administration, 2001

(2) M. DeMerchant, A. Brown, X. Bao and T. Bremner, Structural monitoring by use of a brillouin distributed sensor, Applied Optics, Volume 38, 1999, pp.2755-2759

(3) J. Gao, B. Shi, W. Zhang and H. Zhu, Monitoring the stress of the post-tensioning cable using fiber optic distributed strain sensor, Measurement, Volume 39, 2011, pp.420-428

(4) Z. Wu, B. Xu, K. Hayashi and A. Machida, Distributed optic fiber sensing for a full-scale PC girder strengthened with prestressed PBO sheets, Engineering Structures, Volume 28, 2006, pp.1049-1059

(5) S.K. Kim, Experimental investigation of local damage detection on a 1/15 scale model of a suspension brige deck, KSCE Journal of Civil Engineering, Volume 7, 2003, pp.461-468

(6) H.J. Park, K.Y. Koo and C.B Yun, Modal flexibility-based damage detection technique of steel beam by dynamic strain measurements using FBG sensors, International Journal of Steel Structures, Volume 7, 2007, pp.11-18

(7) J.W. Lee, K.H. Choi and Y.C. Huh, Damage detection method for large structures using static and dynamic strain data from distributed fiber optic sensor, International Journal of Steel Structures, Volume 10, 2010, pp.91-97

(8) F.N. Catbas and A.E. Aktan, Condition and damage assessment: issues and some promising indices, Journal of Structural Engineering, Volume 128, 2002, pp.1026-1036

(9) X.Q. Zhu and S.S. Law, Wavelet-based crack identification of bridge beam from operational deflection time history, International Journal of Solids and Structures, Volume 43, 2006, pp.2299-2317

(10) R.E. Kalman, A new approach to linear filtering and prediction problems, ASME Journal of Basic Engineering, Volume 82, 1960, pp.35-45

(11) K.Y. Wong, Instrumentation and health monitoring of cable-supported bridges, Structural Control and Health Monitoring, Volume 11, 2004, pp.91-124

(12) H.W. Xia, Y.Q. Ni, J.M. Ko and K.Y. Wong, Wavelet-based multi-resolution decomposition of long-term monitoring signal of in-service strain, Proceedings of the 2nd International Postgraduate Conference on Infrastructure and Environment, Hong Kong, 2010, Volume 2, pp.278-285

Acknowledgements

The work described in this paper was supported by The Hong Kong Polytechnic University under Grant No. G-YH47 and through the Development of Niche Areas Programme (Project No. 1-BB68). The writers also wish to thank the Hong Kong SAR Government Highways Department for providing support to this research.